



COMPOSITIONAL HOMOGENEITY OF CM PARENT BODIES

P. VERNAZZA¹, M. MARSSET^{1,2}, P. BECK³, R. P. BINZEL⁴, M. BIRLAN⁵, E. A. CLOUTIS⁶, F. E. DEMEO⁴, C. DUMAS⁷, AND T. HIROI⁸¹Aix Marseille Université, CNRS, LAM (Laboratoire d'Astrophysique de Marseille) UMR 7326, F-13388, Marseille, France; pierre.vernazza@lam.fr²European Southern Observatory (ESO), Alonso de Córdova 3107, 1900 Casilla Vitacura, Santiago, Chile³UJF-Grenoble 1, CNRS-INSU, Institut de Planétologie et d'Astrophysique de Grenoble (IPAG), UMR 5274, Grenoble F-38041, France⁴Department of Earth, Atmospheric, and Planetary Sciences, Massachusetts Institute of Technology, Cambridge, MA 02139, USA⁵IMCCE, Observatoire de Paris, 77 avenue Denfert-Rochereau, F-75014 Paris Cedex, France⁶Department of Geography, University of Winnipeg, Winnipeg, Manitoba R3B 2E9, Canada⁷TMT Observatory, 100 W. Walnut Street, Suite 300, Pasadena, CA 91124, USA⁸Department of Geological Sciences, Brown University, Providence, RI 02912, USA

Received 2016 April 1; revised 2016 May 10; accepted 2016 May 11; published 2016 August 10

ABSTRACT

CM chondrites are the most common type of hydrated meteorites, making up $\sim 1.5\%$ of all falls. Whereas most CM chondrites experienced only low-temperature ($\sim 0^\circ\text{C}$ – 120°C) aqueous alteration, the existence of a small fraction of CM chondrites that suffered both hydration and heating complicates our understanding of the early thermal evolution of the CM parent body(ies). Here, we provide new constraints on the collisional and thermal history of CM-like bodies from a comparison between newly acquired spectral measurements of main-belt Ch/Cgh-type asteroids (70 objects) and existing laboratory spectral measurements of CM chondrites. It first appears that the spectral variation observed among CM-like bodies is essentially due to variations in the average regolith grain size. Second, the spectral properties of the vast majority (unheated) of CM chondrites resemble both the surfaces and the interiors of CM-like bodies, implying a “low” temperature ($< 300^\circ\text{C}$) thermal evolution of the CM parent body(ies). It follows that an impact origin is the likely explanation for the existence of heated CM chondrites. Finally, similarly to S-type asteroids and (2) Pallas, the surfaces of large ($D > 100$ km)—supposedly primordial—Ch/Cgh-type main-belt asteroids likely expose the interiors of the primordial CM parent bodies, a possible consequence of impacts by small asteroids ($D < 10$ km) in the early solar system.

Key words: meteorites, meteors, meteoroids – methods: data analysis – methods: laboratory: solid state – methods: observational – minor planets, asteroids: general – techniques: spectroscopic

1. INTRODUCTION

CM chondrites are phyllosilicate-rich meteorites that make up $\sim 1.5\%$ by number of all falls. Whereas the bulk of each CM chondrite mainly consists of an extremely fine-grained hydrous matrix, these meteorites also comprise high-temperature components (chondrules and CAIs) whose abundance varies widely, from $\sim 50\%$ to 0% in volume (Hutchison 2004), with the lowest fractions being mainly a consequence of the destruction of chondrules during aqueous alteration as well as brecciation.

CM chondrites display a wide range of degrees of aqueous alteration (Brearley 2006; Alexander et al. 2013). Most CM chondrites are classified as petrologic type 2, indicating that they typically have essentially fully hydrated matrices, but within CM2 chondrites, the extent of alteration of chondrules is highly variable from one chondrite to another and is a function of the degree of alteration of the host meteorite and the chondrule type (Hanowski & Brearley 2001). A few CM chondrites exist that show essentially 100% hydration and have been termed CM1 chondrites.

From the hydrated mineralogy and chemistry of CM chondrites (phyllosilicates represent 70%–80% of the volume fraction; Bland et al. 2004; Howard et al. 2009, 2011, 2015), it is believed that they formed from a mixture of water ice and dust and subsequent heating due to the decay of short-lived radioactive nuclides (Urey 1955) led in chronological order to (1) ice melting and (2) aqueous alteration of the dust and thereby formation of secondary phases including phyllosilicates, carbonates and iron oxides which represent most of the volume. It is not yet fully resolved, however, whether the dust

accreted by the CM parent bodies was initially dry or if it had already undergone some aqueous alteration prior to accretion (see Brearley et al. 2006; Zolensky et al. 2008 and references therein). Nevertheless, although preaccretionary alteration may have been important in CM chondrites, its effects have certainly been overprinted by later parent body alteration (Brearley et al. 2006). Finally, whereas most CM chondrites experienced only low temperature ($\sim 0^\circ\text{C}$ – 120°C and certainly less than 300°C ; Dufresne & Anders 1962; Zolensky et al. 1989, 1997; Clayton & Mayeda 1999; Guo & Eiler 2007) aqueous alteration (we call them typical CM chondrites), a low fraction of CM chondrites (Tonui et al. 2014; Nakamura et al. 2015) suffered both hydration and heating (unusual CMs). These meteorites were heated to $> 300^\circ\text{C}$ but questions still remain regarding the mechanism, timing and duration of the heating event (King et al. 2015). Note that Cody et al. (2008) showed that at least one unusual CM, Y 86720, was heated for a very short time (i.e., by an impact).

In parallel to laboratory studies of the spectral properties of both typical and unusual CM chondrites (e.g., Gaffey 1976; Cloutis et al. 2011, 2012; Takir et al. 2013; Beck et al. 2014a; McAdam et al. 2015; Nakamura et al. 2015; Garenne et al. 2016), photometric and spectroscopic observations in the visible and $3\ \mu\text{m}$ wavelength region of main belt asteroids performed over the last 30 years suggest that Ch- and Cgh-type asteroids are the likely parent bodies of CM chondrites (Vilas & Gaffey 1989; Vilas et al. 1993; Lantz et al. 2013; Burbine 2014). These two asteroid types, which represent $\sim 10\%$ of the mass of the asteroid belt (Rivkin 2012; DeMeo & Carry 2013), can be found at all heliocentric distances within the asteroid belt with a

number fraction that appears fairly constant with solar distance, although their abundance may be higher in the middle asteroid belt (2.50–2.82 au) than elsewhere (Bus 1999; Rivkin 2012). An in-depth analysis of the spectral characteristics of the hydration bands of Ch and Cgh types in the visible and 3 μm regions has revealed positive correlations between the asteroid diameter and (1) the depths and/or presence of the 0.7 μm band (Vilas & Sykes 1996, and more recently Fornasier et al. 2014), and (2) the depth of the 3 μm band (Rivkin et al. 2015). Partial dehydration as a consequence of thermal metamorphism in the interior of CM parent bodies has been proposed as a possible explanation for the observed correlations (Fornasier et al. 2014).

Here, we present new spectroscopic observations of 70 Ch- and Cgh-type main belt asteroids and members of four Ch-type families (Adeona, Choris, Dora, Veritas) performed over the near-infrared range (0.7–2.5 μm). This fills in the gap in data between the previously acquired spectra in the visible and 3 μm regions. We utilize this new data set, along with laboratory spectra of CM chondrites from the RELAB database (<http://www.planetary.brown.edu/rehab/>) and data from the University of Winnipeg’s PSF database (<http://psf.uwinnipeg.ca>), to provide new constraints on the early thermal evolution of CM-like bodies. In particular, we use our spectral data to determine whether high temperature ($>300^\circ\text{C}$) metamorphism leading to dehydration did occur in the interiors of the CM parent bodies as a consequence of radiogenic heating.

2. OBSERVATION AND DATA REDUCTION

New data presented here are near-infrared asteroid spectral measurements for Ch- and Cgh-type asteroids from 0.7–2.5 μm obtained using SpeX, the low- to medium-resolution near-IR spectrograph and imager on the 3 m NASA IRTF located on Mauna Kea, HI. Observing runs were conducted remotely primarily from the Observatory of Paris-Meudon, France between 2010 April and 2012 January. The spectrograph SpeX, combined with a 0.8×15 arcsec slit, was used in the low-resolution prism mode for acquisition of the spectra in the 0.7–2.5 μm wavelength range. In order to monitor the high luminosity and variability of the sky in the near-IR, the telescope was moved along the slit during the acquisition of the data so as to obtain a sequence of spectra located at two different positions (A and B) on the array. These paired observations provided near-simultaneous sky and detector bias measurements.

Objects and standard stars were observed near the meridian to minimize their differences in airmass and match their parallactic angle to the fixed N/S alignment of the slit. Our primary solar analog standard stars were 16 Cyg B and Hyades 64. Additional solar analog stars with comparable spectral characteristics were utilized around the sky. Two to three sets of eight spectra per set were taken for each object, each with exposures typically being 120 s. Finally, reduction and telluric correction was performed using a combination of routines within the Image Reduction and Analysis Facility and Interactive Data Language.

In addition, we complemented our data set with additional near-infrared spectra retrieved from the SMASS database (<http://smass.mit.edu/>). Combining these near-infrared measurements with available visible wavelength spectra (Bus 1999; Lazzaro et al. 2004) allows for the first time an extensive visible and near-infrared (VNIR) spectral database of main-belt Ch and Cgh types with $D > 45$ km (78% or 49/63 of all Ch and Cgh types listed in SMASS; see Table 1, Figures 1 and 2).

3. RESULTS

We first performed a detailed analysis of our telescopically measured asteroid spectra. In particular, we focussed on the spectral slope and the ~ 0.7 μm band depth for all objects’ spectra because these two parameters characterize the spectral diversity that is present in our sample especially well. In order to be as complete as possible, we did not restrict our analysis to our sample of VNIR spectra for the calculation of the ~ 0.7 μm band depth, but we also included available visible spectra of the Ch and Cgh types. The ~ 0.7 μm band depth of each asteroid was derived by fitting two fourth-order polynomials to the slope-removed spectrum, one centered at ~ 0.55 μm where the asteroid’s reflectance reaches a local maximum value, and one around the position of the absorption band center at ~ 0.7 μm . The slope was calculated by performing a linear regression to the spectrum. The band depth was then calculated as the difference between the maximum value of the first polynomial and the minimum value of the second one, divided by the maximum value of the first polynomial.

As a second step, we searched for possible correlations between these two parameters and the objects’ physical and dynamical properties, including their diameters, their albedos and their perihelion distances (to test for a change in hydration with heliocentric distance). For all objects with $D > 45$ km, we found significant positive correlations between the diameter and (a) the spectral slope over the visible and near-infrared range (correlation coefficient $r = 0.34$, $N = 49 - a > 98\%$ confidence level that this correlation is not random), (b) the band depth ($r = 0.24$, $N = 86 - a > 97\%$ confidence level that this correlation is not random), and (c) the albedo ($r = 0.38$, $N = 84 - a > 99.9\%$ confidence level that this correlation is not random; see Figure 3). When taking the smaller bodies into account, the correlation remains highly significant only between the diameter and the spectral slope (correlation coefficient $r = 0.51$, $N = 70 - a > 99.9\%$ confidence level that this correlation is not random). Vilas & Sykes (1996) and Fornasier et al. (2014) previously reported a similar correlation between the 0.7 μm band depth and/or presence and the asteroid diameter for $D > 50$ km CM-like asteroids.

As a third step, we performed a detailed comparison of our telescopically measured asteroid spectra with analogous-wavelength laboratory measurements of CM chondrites (Cloutis et al. 2011)—including those that have been heated (Cloutis et al. 2012)—in order to identify plausible explanations for the observed correlations. For typical CM chondrites, we found a highly significant negative correlation (Figure 3) between the average grain size and (a) the spectral slope over the VNIR range ($r = -0.83$, $N = 23 - a > 99.9\%$ confidence level that this correlation is not random; result, in agreement with the findings of Binzel et al. 2015), (b) the band depth (correlation coefficient $r = -0.58$, $N = 23 - a > 99\%$ confidence level that this correlation is not random), and (c) the reflectance at 0.55 μm ($r = -0.64$, $N = 23 - a > 99.9\%$ confidence level that this correlation is not random). Our findings thus support the idea of an anti-correlation between the size of an asteroid and its regolith particle size (Delbo et al. 2007; Delbo & Tanga 2009; Gundlach & Blum 2013). It is interesting to note that the values of the correlation coefficient follow the same trend for asteroids and meteorites (lowest for the 0.7 μm band depth and highest for the spectral slope; Figure 3). A particle-size effect may also explain the observed correlation between the 3 μm band depth and the

Table 1
Observational Circumstances and Spectral Parameters

Asteroid	Observing Date (NIR) ^a	D^b (km)	Albedo ^b (pv)	VNIR slope (μm^{-1})	0.7 μm Band Depth
13	2005 May 19	227.000	0.0690	0.0771865	0.0344054
19	2006 Jan 29	223.000	0.0499	0.192888	0.0364184
34	2004 Feb 20	113.226	0.0543	0.0797893	0.0302174
36	2010 Nov 01	103.000	0.0688	0.130979	0.0396534
38	2011 Jun 06	116.000	0.0617	0.155241	0.0400468
41	2008 May 10	174.000	0.0828	0.110177	0.0264505
48	2005 Oct 08	223.435	0.0615	0.0174509	0.0485328
49	2011 Jan 10	149.800	0.0597	0.0500810	0.0411421
51	2004 Jun 15	142.600	0.0997	0.189472	0.0269757
54	2010 Nov 01	142.000	0.0492	0.0723214	0.0211331
66	2005 Nov 22	71.8200	0.0618	0.101115	0.0228522
70	2010 Nov 01	139.007	0.0397	0.0654554	0.0217925
78	2005 Oct 31	120.600	0.0706	0.119075	0.0244376
91	2011 Oct 21	103.693	0.0404	0.0867205	0.0216958
95	2011 Oct 21	150.189	0.0573	0.110351	0.0312835
105	2010 Nov 01	119.000	0.0466	0.0542794	0.0205865
106	2011 Jan 10	146.590	0.0893	0.104641	0.0356966
111	2004 Sep 22	135.000	0.0600	-0.00119426	0.0323068
112	2011 Oct 20	70.3830	0.0314	0.0504962	0.0102960
121	2012 Jan 24	164.977	0.0773	0.139671	0.0306811
127	2011 Jan 10	129.15	0.042	0.144588	0.0164226
130	2012 Jan 24	198.933	0.0714	0.188504	0.0373451
141	2010 May 10	137.100	0.0493	0.109268	0.0292738
144	2011 Jan 10	142.380	0.0597	0.227307	0.0358152
145	2010 Feb 22	151.000	0.0434	0.0876069	0.0291905
146	2011 Oct 20	131.812	0.0534	0.0675773	0.0188553
156	2011 Oct 21	110.718	0.0504	0.0718514	0.0253548
159	2011 Oct 20	127.434	0.0614	0.0475908	0.0333511
163	2010 Feb 23	81.5790	0.0330	0.123264	0.0274365
194	2011 Oct 21	169.000	0.0524	0.184626	0.0191805
207	2011 Jan 10	61.3130	0.0339	0.0973284	0.0227107
211	2011 Oct 21	143.000	0.0603	0.131072	0.0263804
240	2011 Oct 21	91.3780	0.0531	0.162449	0.0166531
266	2011 Jan 10	109.000	0.0597	-0.0512859	0.0226969
293	2010 Feb 23	57.9010	0.0327	0.0650308	0.0380681
342	2011 Oct 20	64.2660	0.0349	-0.0147895	0.0281876
345	2005 Oct 08	99.0000	0.0591	0.120481	0.0304613
377	2010 May 10	94.0230	0.0555	0.0284047	0.0354600
392	2011 Oct 25	68.9300	0.0542	0.0645685	0.0339383
405	2011 Oct 26	125.000	0.0467	0.174779	0.0455168
410	2010 May 10	118.929	0.0432	0.0135843	0.0294622
490	2010 Sep 04	115.550	0.0622	0.104337	0.0131424
494	2011 Oct 21	86.2820	0.0618	0.0219555	0.0341198
521	2010 Feb 22	111.250	0.0677	0.180916	0.0296534
586	2012 Jan 21	82.3700	0.0539	0.0451591	0.0386582
668	2010 May 10	22.5545	0.05755	0.121436	0.0315906
706	2006 Jan 30	29.2200	0.1721	0.176127	0.0517200
735	2011 Oct 21	70.6990	0.0535	0.0129118	0.0397391
776	2005 Apr 12	151.113	0.0655	0.111122	0.0297223
910	2011 Oct 26	50.7560	0.0308	0.0454414	0.0112490
997	2010 May 10	20.3910	0.0572	0.150611	0.0467839
1086	2011 Oct 20	79.8670	0.0528	0.0463236	0.0306125
1384	2010 Feb 23	29.5920	0.0351	0.107045	0.0439743
1403	2010 Feb 22	27.2840	0.0655	0.0637682	0.0134371
1734	2011 Oct 20	27.1300	0.0492	0.0325078	0.0294833
1783	2010 Sep 04	24.2680	0.0546	0.0241756	0.0364861
1795	2010 Feb 23	24.5210	0.0310	-0.0672690	0.0120872
1936	2010 May 10	33.8045	0.0302	0.0925063	0.0628857
1970	2010 May 10	20.6950	0.0489	0.00489748	0.0242104
2378	2005 May 11	40.3730	0.0569	0.0574032	0.0197925
2428	2011 Oct 20	23.6520	0.115	0.00764904	0.0389953
2598	2010 Feb 23	15.6940	0.0491	-0.0958053	0.0305925
2807	2011 Oct 20	16.8660	0.0566	-0.00491424	0.0181475
2934	2010 Sep 03	21.9410	0.110	-0.0632008	0.0580830

Table 1
(Continued)

Asteroid	Observing Date (NIR) ^a	D^b (km)	Albedo ^b (pv)	VNIR slope (μm^{-1})	0.7 μm Band Depth
3611	2010 Feb 23	14.0440	0.0435	-0.0576519	0.0325344
3775	2010 Sep 04	17.0910	0.0365	-0.0369834	0.0865412
5348	2010 Nov 01	15.17	0.070	-0.0158047	0.0339880
5416	2010 Sep 04	19.0060	0.0358	-0.0120133	0.00268611
5592	2010 May 11	22.3745	0.0711	-0.0907577	0.00472240
7868	2010 Sep 04	15.9080	0.0395	0.0516513	0.00107513

Notes. The signal-to-noise ratio for most asteroid spectra is generally above 100, and above 50 for all objects.

^a For observations reported here, we give the observation date (UT). All near-infrared (NIR) data were obtained using the NASA IRTF at Mauna Kea, Hawaii.

^b Albedo and diameters were taken from *IRAS* and/or *WISE* (Masiero et al. 2011, 2012).

asteroid diameter (Rivkin et al. 2015). The few available laboratory spectra of CM chondrites in this wavelength range support this hypothesis, with fine-grained spectra displaying deeper 3 μm bands with respect to coarse-grained spectra (See Figure 4).

If the above interpretation is correct, one should observe the same anti-correlation between the regolith grain size and the asteroid diameter among other asteroid classes including among the well-studied S-type asteroids. In order to avoid any effect due to composition, we performed such investigation for olivine-rich, metal-poor LL-like asteroids thus avoiding the band depth reducing effect of metal among the metal-rich H-like bodies. Note that we have previously performed the analysis of their spectral properties (Vernazza et al. 2008, 2014) and the present investigation only required using the best-fit values derived at that time with a radiative transfer model (Shkuratov et al. 1999). In the previous studies, we found a highly significant negative correlation between the grain size derived by our model (the model output is actually the optical pathlength which is proportional to the grain size) and the asteroid diameter ($r = -0.66$, $N = 55 - a > 99.9\%$ confidence level that this correlation is not random), thus validating the above interpretation (Figure 5).

We therefore find, on average, that the reflectance spectra of fine-grained ($<100 \mu\text{m}$) typical CM chondrites closely reproduce the reflectance properties of the largest ($D > 100 \text{ km}$) CM-like asteroids (higher albedo, redder slope and deeper 0.7 μm bands), whereas the spectra of coarser grained (100–200 μm) typical CM chondrites appear to better match the spectral properties of smaller-sized ($D < 60 \text{ km}$) CM-like asteroids (lower albedo, bluer slope and shallower 0.7 μm bands; Figure 6).

We notice, however, that the derived slope, 0.7 μm band depth, and albedo values for our asteroid sample are slightly shifted with respect to the meteorite ones, implying that an additional effect is operating on asteroids. On average, the asteroid spectra are bluer and possess shallower 0.7 μm band depths. These two differences are consistent with laboratory experiments that simulate the space weathering effects of micrometeorite bombardment (Matsuoka et al. 2015) and vacuum exposure of serpentinite (Cloutis et al. 2008), solar wind ion irradiation having little influence on the spectral properties of CM chondrites (Lantz et al. 2015). Note that it is difficult to interpret the difference between the asteroid albedos and meteorite reflectances given that these two quantities are not directly equivalent. Space weathering effects may also explain the fact that the smaller ($D < \sim 30 \text{ km}$) CM-like asteroids possess, on average, deeper 0.7 μm bands. Indeed,

their surfaces being younger (small asteroids possess shorter collisional lifetimes with respect to larger ones), the space-weathering effects caused by the bombardment of micrometeorites have not had time to operate.

The consequence of these smaller objects ($D < \sim 30 \text{ km}$) possessing, on average, deeper 0.7 μm bands is that the average slope removed spectrum of $D < 60 \text{ km}$ Ch/Cgh-type asteroids is nearly identical to the average spectrum for $D > 100 \text{ km}$ bodies (Figure 7). Interestingly, while many $D < \sim 60 \text{ km}$ sized bodies are likely collisional fragments (Bottke et al. 2005; Consolmagno et al. 2008; Morbidelli et al. 2009; Carry 2012, and references therein) representing the interiors of the original potential CM parent body(ies), large bodies ($D > 100 \text{ km}$) are more likely to be largely intact survivors capable of preserving at least some of their original surface materials. Our results thus imply no significant compositional difference between the surface ($D > 100 \text{ km}$) and the interior ($D < 60 \text{ km}$) for the potential parent bodies of CM chondrites, both (interior and surface) being compatible with the vast majority of the CM chondrites (namely, typical CMs).

Finally, a direct comparison of our asteroid spectra with those of the heated CM chondrites indicates that these meteorites can only make up small proportions ($<10\%$) of the asteroid surfaces (Figure 8). In particular, there is no evidence of this material being more abundant in the interiors ($D < 60 \text{ km}$) than at the surfaces ($D > 100 \text{ km}$) of primordial CM-like bodies.

4. IMPLICATIONS

4.1. Anti-correlation between the Size of an Asteroid and its Regolith Grain Size

On the basis of an in-depth analysis of the visible and near-infrared spectral properties of CM-like (Ch and Cgh types) asteroids, we found a positive correlation between various parameters (spectral slope, 0.7 μm band depth, asteroid albedo) and the asteroid diameter. We analyzed the visible and near-infrared spectral properties of classical CM chondrites in the same way and found a negative correlation between these same parameters (spectral slope, 0.7 μm band depth, reflectance at 0.55 μm) and the grain size of the sample. These trends suggest that for CM-like asteroids, there is an anti-correlation between the asteroid diameter and the regolith grain size. To test whether or not this anti-correlation is independent of the asteroid surface composition, we searched for a similar trend among the S-type asteroids with an LL-like composition. We found that the anti-correlation is also highly significant for these objects, suggesting that our findings are global. It

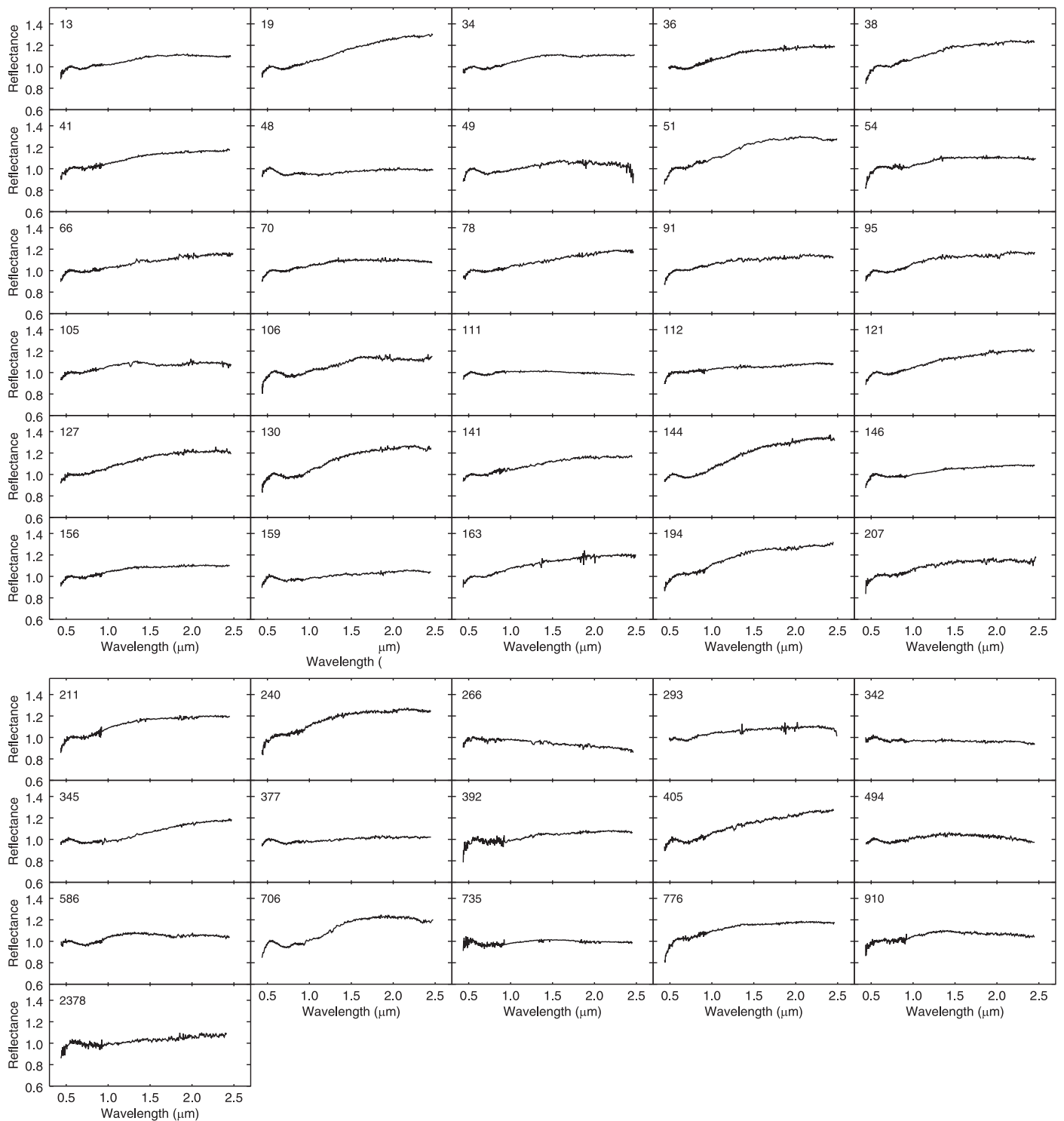


Figure 1. Plots of the final reduced NIR spectra of Ch/Cgh-type asteroids (non-family members) presented in this paper combined with available visible wavelength spectra (Bus 1999; Lazzaro et al. 2004). The asteroid number is indicated on each plot.

therefore appears that the spectral variability observed among CM-like asteroids is mainly due to a variation of the average regolith grain size rather than to different thermal histories (Fornasier et al. 2014; Rivkin et al. 2015).

Our findings are consistent with evidence that have been accumulated over the years in support of an anti-correlation between regolith grain size and asteroid diameter. The first indications that this might be the case came from polarization

measurements (Dollfus & Zellner 1979 and references therein) that showed that the moon and Vesta possess fine-grained regoliths. Later on, a survey of the spectral properties of S-type asteroids (Gaffey et al. 1993) revealed a correlation between band depth and diameter, but grain size was not recognized at the time as the main cause of the spectral variability. In the mid-infrared range, measurements of the thermal inertia revealed an anti-correlation between the regolith grain size

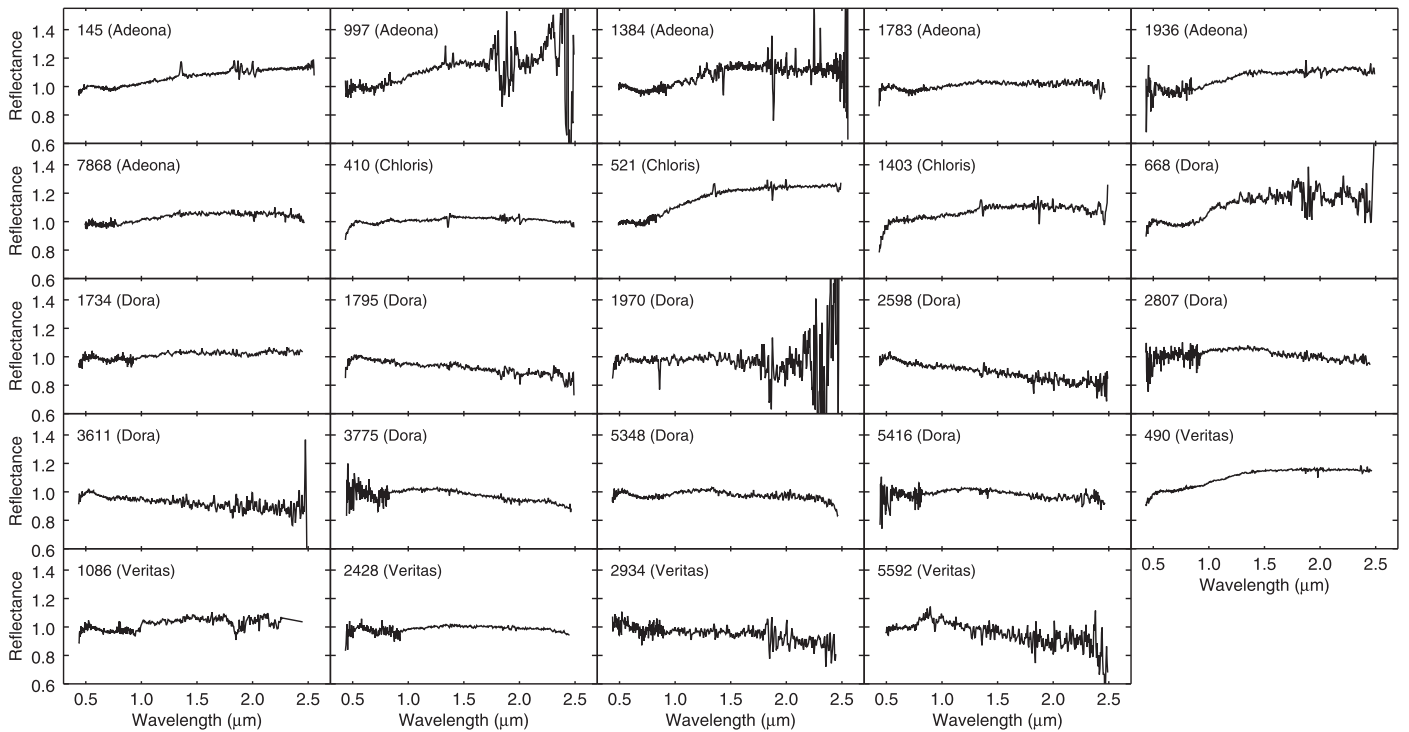


Figure 2. Plots of the final reduced NIR spectra of Ch/Cgh-type asteroids (family members; name of the collisional family is indicated in parenthesis) presented in this paper combined with available visible wavelength spectra (Bus 1999; Lazzaro et al. 2004).

and the gravitational acceleration (i.e., diameter) of an asteroid (Delbo et al. 2007; Delbo & Tanga 2009; Gundlach & Blum 2013). In addition, it was shown that such an anti-correlation is independent of the asteroid spectral class (Gundlach & Blum 2013). In this same wavelength range, a spectral variability for differently sized compositionally similar asteroids was noticed (Vernazza et al. 2010) and interpreted as being caused by different particle size distributions. Space missions have provided the most recent piece of evidence along these lines. The regolith of the S-type asteroid Itokawa ($D \sim 0.3$ km; Demura et al. 2006) regolith appears to be dominated in number by grains >1 mm in size (Miyamoto et al. 2007), whereas the surfaces of larger asteroids such as Lutetia ($D \sim 98$ km; Sierks et al. 2011) and Vesta ($D \sim 525$ km; Jaumann et al. 2012; Russell et al. 2012) appear to be covered by finer-grained regolith that are similar to that of the moon (Hiroi et al. 1994; Coradini et al. 2011; Jaumann et al. 2012; Vincent et al. 2012). That said, the Itokawa regolith particles that were returned to Earth are fine-grained (size range between 3 and $180 \mu\text{m}$, but most are $<10 \mu\text{m}$, Nakamura et al. 2011).

It thus appears that for interpreting correctly the surface composition of asteroids, one needs to use laboratory spectral measurements of compositionally analogous materials collected with the appropriate grain size range. For $D > 100$ km asteroids, a grain size range of $\sim 0\text{--}50 \mu\text{m}$ would be the most appropriate, whereas for $D < 100$ km, one should use spectra collected for particle sizes in the $\sim 50\text{--}200 \mu\text{m}$ range. For the IDP-like C-, P-, and D-type asteroids (Vernazza et al. 2015), excluding Ch and Cgh types analyzed here, one should use a grain size range of $\sim 0\text{--}2 \mu\text{m}$.

Finally, as discussed in Gundlach & Blum (2013), the decrease in regolith grain size with increasing asteroid diameter can be qualitatively understood as a natural consequence of the

collisional history of the asteroids. Indeed, since for a given impact the smaller grains reach the highest velocities (Fujiwara & Tsukamoto 1980; Vickery 1986, 1987; Nakamura & Fujiwara 1991; Nakamura 1993; Nakamura et al. 1994), it is expected that these velocities will exceed the escape velocity in the case of the smaller bodies whereas larger bodies will have sufficient gravity to retain the smallest particles. Also, the collisional lifetime of an asteroid being inversely proportional to its size, smaller asteroids possess, on average, much younger surfaces than larger ones, their surfaces being reset more frequently via collisions. The formation of fine regolith grains either via impacts or thermal fatigue fragmentation (Delbo et al. 2014) being a time-dependent process, it is thus expected that larger asteroids will possess, on average, a higher fraction of fine grained material at their surfaces compared to smaller asteroids.

4.2. Low Temperature Thermal Evolution for the CM Parent Bodies

Here, we found that the spectral properties of Ch- and Cgh-type asteroids, including those of the family members, appear very similar to those of the vast majority of CM chondrites. In particular, the spectral properties of the unusual heated CM chondrites appear globally inconsistent with those of our asteroid sample, implying that these meteorites can only represent a small fraction of the surface material of CM-like bodies. This is in agreement with their low abundance among CM falls and finds. The spectral properties of Ch- and Cgh-type asteroids thus argue against extensive heating of CM-like bodies. Consequently, the vast majority of CM chondrites closely resemble both the surfaces and the interiors of CM-like bodies.

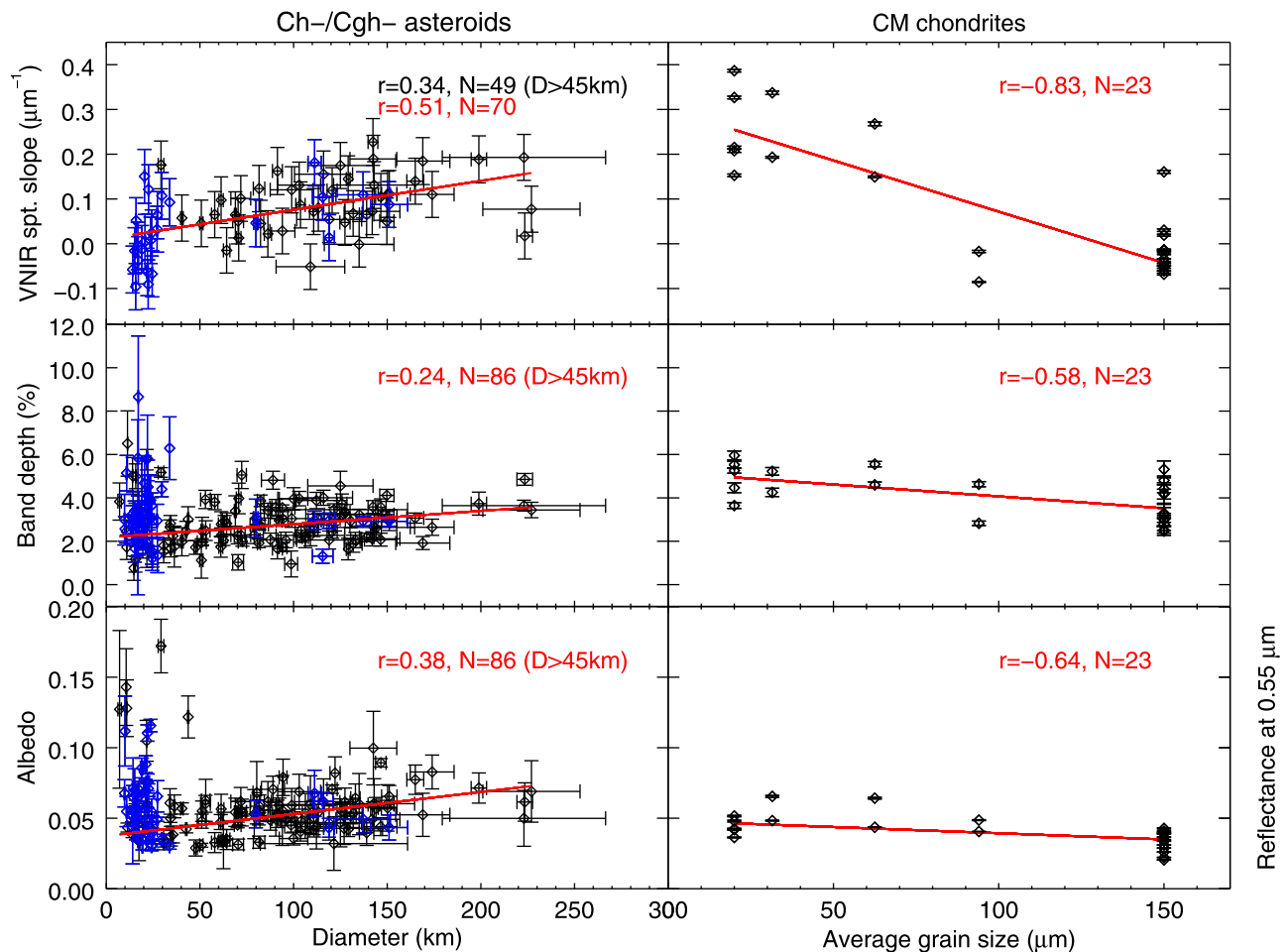


Figure 3. Comparison between the spectral properties of CM-like asteroids and those of classical CM chondrites. (left) For $D > 45$ km Ch-/Cgh-type asteroids, we observe a statistically significant positive linear relation between the diameter and (1) slope, (2) $0.7 \mu\text{m}$ band depth, and (3) geometric albedo. Non-family members are labelled in black whereas family members appear in blue. (right) For classical CM chondrites, we observe a statistically significant negative linear relation between the average grain size and (1) slope, (2) $0.7 \mu\text{m}$ band depth, and (3) reflectance at $0.55 \mu\text{m}$. The average grain size was taken half way between two sieve sizes. From left to right, the sieve sizes were as following: 0–40, 0–63, 0–125, 63–125 μm , and 100–200 μm . In all cases, the number of points (N) and the correlation coefficient (r) are indicated on the plot.

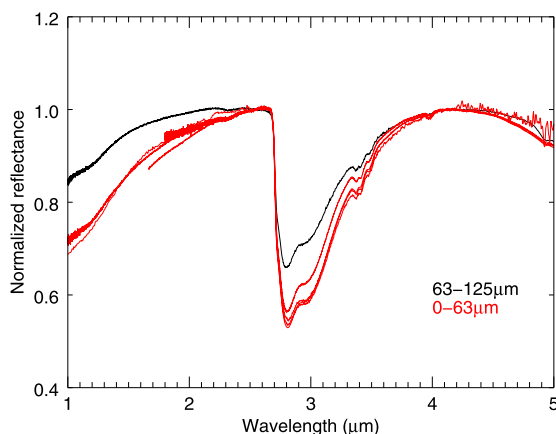


Figure 4. $3 \mu\text{m}$ band of CM chondrites as a function of grain size. The spectra were collected at RELAB. Samples with smaller grain sizes yield deeper $3 \mu\text{m}$ bands with respect to coarse-grained samples. It is important to stress that there are few measurements available in this wavelength range.

From the present study, it seems unlikely that the heated CMs originate from the cores of CM-like bodies where they would have been heated via the decay of short-lived radionuclides during the early history of the solar system. If this

would have been the case, this would imply that the interior of CM-like bodies once reached peak temperatures of $\sim 500^\circ\text{C}$ – 700°C (this is the estimated peak temperature for a number of heated CMs, Tonui et al. 2014; King et al. 2015) and a consequence of such peak temperature would be—following current thermal models—that most of the interior volume (up to 10–20 km below the surface) of CM-like bodies would have been heated to high temperatures as well (e.g., Grimm & McSween 1989; Cohen & Coker 2000; Castillo-Rogez & Schmidt 2010; Schmidt & Castillo-Rogez 2012). Yet this is neither consistent with our spectral data nor with the properties of CM chondrites where heated CMs represent only a small fraction of all CM chondrites.

An alternative and more likely hypothesis is that the heated CM chondrites formed via impacts over the course of solar system history. Short duration thermal metamorphism through hypervelocity impacts has the potential to dehydrate the phyllosilicates (Beck et al. 2014b). Such a phenomenon has been observed in impact experiments conducted on serpentine minerals (Akai & Kanno 1986), and similar behavior has been observed during shock experiments on Murchison (e.g., Tyburczy et al. 1986; Tomeoka et al. 1999). Importantly, the fact that the organic matter in CM chondrites shows a structural

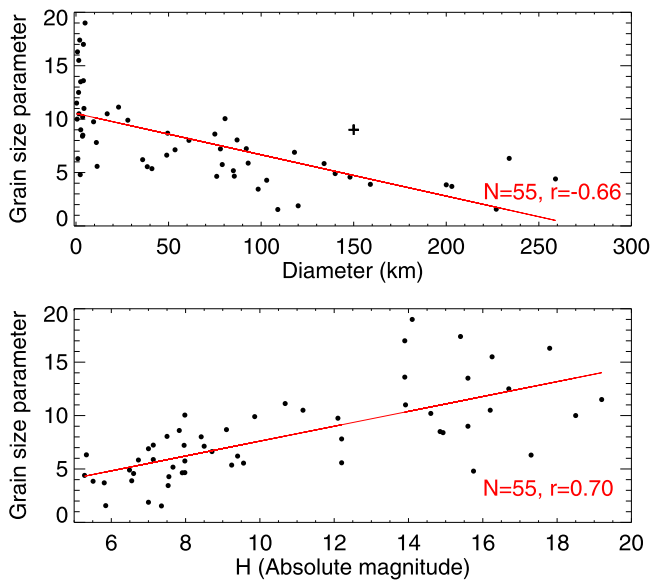


Figure 5. Anti-correlation between regolith grain size and asteroid diameter for LL-like S-type asteroids. For LL-like S-type asteroids, we observe a statistically significant negative linear relation between the diameter and the average regolith grain size (top), and thus a positive linear relation between the H magnitude and the average regolith grain size (bottom).

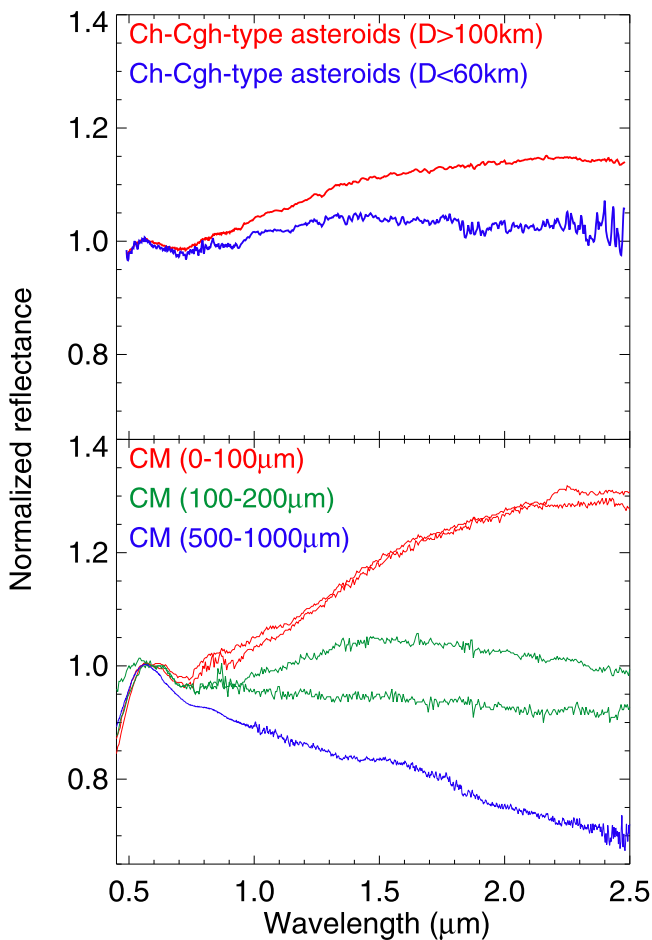


Figure 6. Anti-correlation between regolith grain size and asteroid diameter for CM-like asteroids. The spectral properties of large ($D > 100$ km; 34 objects) asteroids (top) follow, on average, the same trend as those of fine-grained CM chondrites (bottom). Reciprocally, the spectral properties of the smaller ($D < 60$ km; 23 objects) asteroids (top) follow, on average, the same trend as those of coarse-grained (grain size $> 100 \mu\text{m}$) CM chondrites (bottom).

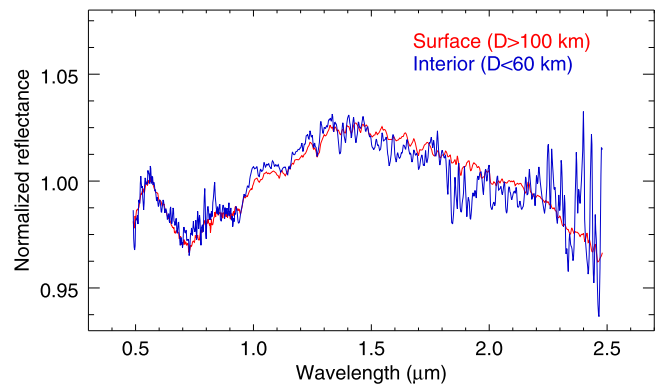


Figure 7. Comparison between the average spectral properties of the small ($D < 60$ km) and large ($D > 100$ km) Ch/Cgh-type asteroids after slope removal. Both the absence of any spectral difference—apart from the spectral slope—between the large and small Ch/Cgh-type asteroids and the fact that these objects have spectral properties compatible with those of typical unheated CM chondrites implies: (1) a compositional homogeneity of CM parent bodies, and (2) a “low” temperature ($< 300^\circ\text{C}$) thermal evolution of the CM parent bodies.

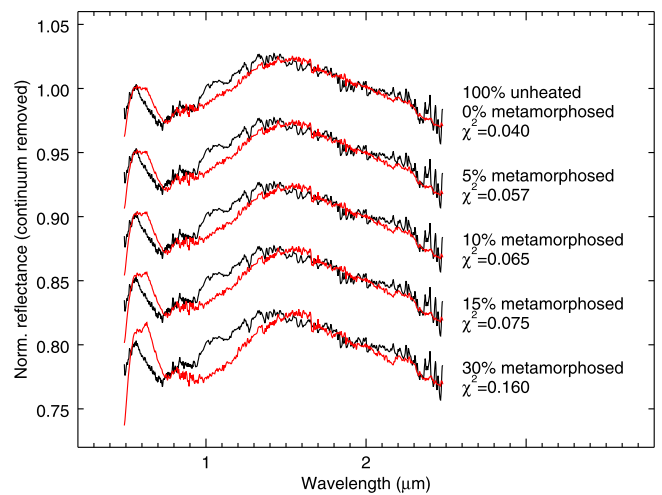


Figure 8. Comparison between the average spectrum of Ch/Cgh-type asteroids (after slope removal) and a best fit using several CM chondrites (unheated and heated) spectra as input. The best fit is obtained for a linear mixture of unheated CM chondrites. When imposing an increasing fraction of metamorphosed CM chondritic material, the chi-square becomes worse. This minimizes the presence of metamorphosed CM chondrite material at the surfaces of CM-like bodies.

evolution different from that experienced by ordinary chondrites (Quirico et al. 2014) seems to point toward impact heating as the heat source (this applies also to heated CR chondrites; Briani et al. 2013). Also, some evidence for short-duration heating are present in the form of exciton in the Carbon XANES spectra (Cody et al. 2008) of one heated CM chondrite and is reproduced by flash heating experiments. This would tend to support impact metamorphism as a heat source. In summary, impact alteration products would seem the likely explanation for the heated CM chondrites and would naturally explain their low abundance among CM falls and finds. Concerning the early thermal evolution of CM-like Ch- and Cgh-type asteroids, it likely occurred at low temperature so that both the near surface and interior of these bodies resemble the typical relatively unheated and phyllosilicate-rich CM chondrites. These constraints will serve as input to models attempting to reproduce the early thermal evolution of CM-like bodies.

Finally, this study has shown that one has to be careful when using the depth of the 0.7 and 3 μm bands when assessing the thermal histories of phyllosilicate-rich CM-like bodies. The latter appears to be anti-correlated with grain size in the case of a CM composition and thus positively correlated with the size of the asteroid. Thus, shallow 0.7 and/or 3 μm bands are not necessarily indicative of dehydration. Along these lines, McAdam et al. (2015) have recently shown that the presence of a 0.7 μm charge transfer band is an indicator of aqueous alteration, but is insensitive to the degree of alteration. They have also shown that some CM/CI meteorites, which range in alteration from 60 to 90 vol.% phyllosilicates, do not have a charge transfer band, implying that multi-wavelength observations of asteroids are crucial for determining both the state and degree of aqueous alteration.

4.3. Surfaces of CM-like Asteroids as Exposed Interiors?

Our observations of phyllosilicate-rich surface compositions for present-day $D > 100$ km CM-like asteroids is unexpected since thermal evolution models for CM-like bodies and more generally for small bodies ($D < 300$ km) that accreted from a mixture of dust and ice predict, as a direct consequence of radiogenic heating, the formation of a body consisting of (1) a primordial ~ 6 –15 km thick outer shell that did not experience aqueous alteration (i.e., that remained frozen), and (2) an aqueously altered interior (e.g., Grimm & McSween 1989; Cohen & Coker 2000; Young 2001; Brearley 2006, pp. 584–624; Palaguta et al. 2010). As such, the surface material we observe today on large ($D > 100$ km) CM-like bodies is consistent with a formation in the interior of once larger bodies if one assumes that the dust prior to accretion was dry. In this case, a natural explanation for the surfaces of supposedly primordial (collisionally undisrupted) $D > 100$ km CM-like asteroids consisting mostly of material formed in the interior (hydrated silicates), is that impacts by asteroids over the course of solar system history, and in particular those that occurred during the first ~ 20 Myr of solar system formation (Ciesla et al. 2013), brought deep material up to the surface. One can also not exclude that the surfaces were progressively stripped away revealing the altered material below it. Such collisional histories for CM-like bodies is supported by the fact that all CM chondrites studied by Bischoff & Schultz (2004) and Bischoff et al. (2006, pp. 679–712) were classified as regolith breccias. Note that similar collisional histories have been predicted for S-type asteroids (Vernazza et al. 2014). Such a collisional history would also be consistent with the hydrated surface composition of (2) Pallas (e.g., Hiroi et al. 1996; Rivkin et al. 2003) and the suggestion that this object lost its primordial icy crust following impacts as proposed by Schmidt & Castillo-Rogez (2012). If the dust particles prior to accretion were already hydrated as advocated by Metzler et al. (1992) and Bischoff (1998), then the need to invoke an intense post-accretionary collisional evolution would be alleviated. However, the textural evidence in CM chondrites for hydration prior to accretion is weak at best (Brearley 2006, pp. 584–624).

Importantly, a similar observation is not made in the case of many C-, P-, and D-type asteroids that seem to have preserved at least part of their primordial outer shell. This is deduced both from the absence of a 3 μm feature in their spectra (e.g., Emery & Brown 2003; Rivkin et al. 2003; Takir & Emery 2012) combined with the presence of fine-grained anhydrous silicates at their surfaces (e.g., Emery et al. 2006; Vernazza et al. 2012,

2015; Marsset et al. 2016). Altogether, these observations would support the idea (1) that ordinary chondrite and CM chondrite parent bodies experienced a more violent collisional history than C-, P-, and D-type (IDP-like) asteroids, or (2) that the IDP-like (C, P, D) asteroids possessed a much thicker primordial outer shell with respect to CM-like bodies, possibly as a consequence of a later accretion and/or longer duration of accretion. Both cases would argue in favor of different formation locations for CM-like and IDP-like bodies (e.g., Walsh et al. 2011).

5. CONCLUSION

We conducted an extensive spectroscopic survey in the near-infrared range of 70 main-belt Ch/Cgh-type asteroids and 4 Ch/Cgh-type families and combined these measurements with available visible wavelength spectra. A detailed comparison of the spectral properties of our asteroid sample with those of their meteoritic analog (CM chondrites) first allowed us to constrain the origin of the spectral variation observed among Ch/Cgh types. The latter is coherent with fine-grained CM-like regolith being present at the surfaces of the largest bodies and coarse-grained CM-like regolith being present at the surfaces of the smaller bodies. This anti-correlation between the asteroid diameter and the average regolith grain size is coherent with previous measurements in the thermal infrared. A proper understanding of the spectral variation among CM-like asteroids further allowed us to reach the following conclusions regarding their collisional and thermal history.

- (1) The spectral properties of Ch- and Cgh-type asteroids including those of the family members appear very similar to those of the vast majority (unheated) CM chondrites. In particular, the spectral properties of the less common thermally metamorphosed CM chondrites appear globally inconsistent with those of our asteroid sample implying that these meteorites can only represent a small fraction of the surface material of CM-like bodies, in agreement with their low abundance among CM falls and finds. The spectral properties of Ch- and Cgh-type asteroids thus argue against heavy thermal evolution of CM-like bodies. The latter must have occurred at low temperature ($< 300^\circ\text{C}$), and consequently the vast majority of CM chondrites reflect well both the surface and the interior of CM-like bodies. Finally, an impact origin for heated CM chondrites is favored by our observations.
- (2) The CM-like surfaces of the largest ($D > 100$ km)—supposedly primordial—Ch/Cgh-type asteroids are coherent with being exposed interiors if one assumes that the dust from which the CM parent bodies accreted was mostly dry. A similar conclusion has been reached in the past in the cases of S-type asteroids (Vernazza et al. 2014) and (2) Pallas (Schmidt & Castillo-Rogez 2012). However, a similar observation is not made in the case of many IDP-like C-, P-, and D-type asteroids that seem to have preserved at least part of their primordial outer shell. This apparent dichotomy favors different formation locations for CM-like and IDP-like bodies.

We warmly thank the referee for a very constructive review. Part of the data utilized in this publication were obtained and made available by the The MIT-UH-IRTF Joint Campaign for NEO Reconnaissance. The IRTF is operated by the University of

Hawaii under Cooperative Agreement No. NCC 5-538 with the National Aeronautics and Space Administration, Office of Space Science, Planetary Astronomy Program. The MIT component of this work is supported by NASA grant 09-NEOO009-0001, and by the National Science Foundation under grants Nos. 0506716 and 0907766. F.E.D. acknowledges support from NASA under grant No. NNX12AL26G issued through the Planetary Astronomy Program. E.A.C. thanks the Canada Foundation for Innovation, the Manitoba Research Innovations Fund, the Canadian Space Agency, the University of Winnipeg, and the Natural Sciences and Engineering Research Council of Canada for supporting the establishment and operation of the University of Winnipeg's Planetary Spectrophotometer Facility and this study.

REFERENCES

- Akai, J., & Kanno, J. 1986, *PolRe*, **41**, 259
- Alexander, C. M. O.'D., Howard, K. T., Bowden, R., & Fogel, M. L. 2013, *GeCoA*, **123**, 244
- Beck, P., Garenne, A., Quirico, E., et al. 2014a, *Icar*, **229**, 263
- Beck, P., Quirico, E., Garenne, A., et al. 2014b, *M&PS*, **49**, 2064
- Binzel, R. P., DeMeo, F. E., Burt, B. J., et al. 2015, *Icar*, **256**, 22
- Bischoff, A. 1998, *M&PS*, **33**, 1113
- Bischoff, A., & Schultz, L. 2004, in Proc. 67th Annual Meeting of the Meteoritical Society abstract no. 5118, *Meteoritics & Planetary Science* 39, Supplement
- Bischoff, A., Scott, E. R. D., Metzler, K., & Goodrich, C. A. 2006, in *Meteorites and the Early Solar System II*, ed. D. S. Lauretta, & H. Y. McSween, Jr. (Tucson, AZ: Univ. Arizona Press)
- Bland, P. A., Cressey, G., & Menzies, O. N. 2004, *M&PS*, **39**, 3
- Bottke, W. F., Durda, D. D., Nesvorný, D., et al. 2005, *Icar*, **175**, 111
- Brearley, A. J. 2006, in *Meteorites and the Early Solar System II*, ed. D. S. Lauretta, & H. Y. McSween, Jr. (Tucson, AZ: Univ. Arizona Press)
- Briani, G., Quirico, E., Gounelle, M., et al. 2013, *GeCoA*, **122**, 267
- Burbine, T. H. 2014, in *Treatise on Geochemistry*, Vol. 2 ed. A. M. Davis (2nd ed.; Amsterdam: Elsevier)
- Bus, S. J. 1999, PhD Thesis, Massachusetts Inst. Technol.
- Carry, B. 2012, *P&SS*, **73**, 98
- Castillo-Rogez, J. C., & Schmidt, B. E. 2010, *GeoRL*, **37**, L10202
- Ciesla, F. J., Davison, T. M., Collins, G. S., & O'Brien, D. P. 2013, *M&PS*, **48**, 2559
- Clayton, R. N., & Mayeda, T. K. 1999, *GeCoA*, **63**, 2089
- Cloutis, E. A., Craig, M. A., Kruzelecky, R. V., et al. 2008, *Icar*, **195**, 140
- Cloutis, E. A., Hudon, P., Hiroi, T., & Gaffey, M. J. 2012, *Icar*, **220**, 586
- Cloutis, E. A., Hudon, P., Hiroi, T., Gaffey, M. J., & Mann, P. 2011, *Icar*, **216**, 309
- Cody, G. D., Alexander, C. M. O.'D., Yabuta, H., et al. 2008, *E&PSL*, **272**, 446
- Cohen, B. A., & Coker, R. A. 2000, *Icar*, **145**, 369
- Consolmagno, G. J., Britt, D. T., & Macke, R. J. 2008, *ChEG*, **68**, 1
- Coradini, A., Capaccioni, F., Erard, S., et al. 2011, *Sci*, **334**, 492
- Delbo, M., dell'Oro, A., Harris, A. W., Mottola, S., & Mueller, M. 2007, *Icar*, **190**, 236
- Delbo, M., Libourel, G., Wilkerson, J., et al. 2014, *Natur*, **508**, 233
- Delbo, M., & Tanga, P. 2009, *Sci*, **57**, 259
- DeMeo, F. E., & Carry, B. 2013, *Icar*, **226**, 723
- Demura, H., Kobayashi, S., Nemoto, E., et al. 2006, *Sci*, **312**, 1347
- Dollfus, A., & Zellner, B. H. 1979, *Asteroids* (Tucson, AZ: Univ. Arizona Press), 170
- Dufresne, E. R., & Anders, E. 1962, *GeCoA*, **26**, 1085
- Emery, J. P., & Brown, R. H. 2003, *Icar*, **164**, 104
- Emery, J. P., Cruikshank, D. P., & van Cleve, J. 2006, *Icar*, **182**, 496
- Fornasier, S., Lantz, C., Barucci, M. A., & Lazzarin, M. 2014, *Icar*, **233**, 163
- Fujiwara, A., & Tsukamoto, A. 1980, *Icar*, **44**, 142
- Gaffey, M. J. 1976, *JGR*, **81**, 905
- Gaffey, M. J., Bell, J. F., Brown, R. H., et al. 1993, *Icar*, **106**, 573
- Garenne, A., Beck, P., Montes-Hernandez, G., et al. 2016, *Icar*, **264**, 172
- Grimm, R. E., & McSween, H. Y., Jr. 1989, *Icar*, **82**, 244
- Gundlach, B., & Blum, J. 2013, *Icar*, **223**, 479
- Guo, W., & Eiler, J. M. 2007, *GeCoA*, **71**, 5565
- Hanowski, N. P., & Brearley, A. J. 2001, *GeCoA*, **65**, 495
- Hiroi, T., Pieters, C. M., & Takeda, H. 1994, *M&PS*, **29**, 394
- Hiroi, T., Zolensky, M. E., Pieters, C. M., & Lipschutz, M. E. 1996, *M&PS*, **31**, 321
- Howard, K. T., Alexander, C. M. O.'D., Schrader, D. L., & Dyl, K. A. 2015, *GeCoA*, **149**, 206
- Howard, K. T., Benedix, G. K., Bland, P. A., & Cressey, G. 2009, *GeCoA*, **73**, 4576
- Howard, K. T., Benedix, G. K., Bland, P. A., & Cressey, G. 2011, *GeCoA*, **75**, 2735
- Hutchison, R. 2004, *Meteorites: A Petrologic, Chemical and Isotopic Synthesis* (Cambridge: Cambridge Univ. Press)
- Jaumann, R., Williams, D. A., Buczkowski, D. L., et al. 2012, *Sci*, **336**, 687
- King, A. J., Schofield, P. F., & Russell, S. S. 2015, in 78th Annual Meeting of the Meteoritical Society, LPI Contribution No. 1856, *Thermal Alteration of CI and CM Chondrites: Mineralogical Changes and Metamorphic Temperatures*, 5212
- Lantz, C., Brunetto, R., Barucci, M. A., et al. 2015, *A&A*, **577**, 9
- Lantz, C., Clark, B. E., Barucci, M. A., & Lauretta, D. S. 2013, *A&A*, **554**, 7
- Lazzaro, D., Angeli, C. A., Carvano, J. M., et al. 2004, *Icar*, **172**, 179
- Marsset, M., Vernazza, P., Birlan, M., et al. 2016, *A&A*, **586**, 9
- Masiero, J. R., Mainzer, A. K., Grav, T., et al. 2011, *ApJ*, **741**, 68
- Masiero, J. R., Mainzer, A. K., Grav, T., Bauer, J. M., & Jedicke, R. 2012, *ApJ*, **759**, 14
- Matsuoka, M., Nakamura, T., Kimura, Y., et al. 2015, *Icar*, **254**, 135
- McAdam, M. M., Sunshine, J. M., Howard, K. T., & McCoy, T. M. 2015, *Icar*, **245**, 320
- Metzler, K., Bischoff, A., & Stöffler, D. 1992, *GeCoA*, **56**, 2873
- Miyamoto, H., Yano, H., Scheeres, D. J., et al. 2007, *Sci*, **316**, 1011
- Morbidelli, A., Bottke, W. F., Nesvorný, D., & Levison, H. F. 2009, *Icar*, **204**, 558
- Nakamura, A. 1993, *Laboratory Studies on the Velocity of Fragments from Impact Disruptions*, ISAS Rep. 651 (Sagamihara: Tokyo Univ.)
- Nakamura, A., & Fujiwara, A. 1991, *Icar*, **92**, 132
- Nakamura, A. M., Fujiwara, A., & Kadono, T. 1994, *P&SS*, **42**, 1043
- Nakamura, T. 2005, *JMPeS*, **100**, 260
- Nakamura, T., Iwata, T., Kitasato, K., et al. 2015, in 78th Annual Meeting of the Meteoritical Society, LPI Contribution No. 1856, *Reflectance Spectra Measurement of Various Carbonaceous Chondrites Using Hayabusa-2 Near Infrared Spectrometer*, 5206
- Nakamura, T., Noguchi, T., Tanak, M., et al. 2011, *Sci*, **333**, 1113
- Palguta, J., Schubert, G., & Travis, B. 2010, *E&PSL*, **296**, 235
- Quirico, E., Orthous-Daunay, F., Beck, P., et al. 2014, *GeCoA*, **136**, 80
- Rivkin, A. S. 2012, *Icar*, **221**, 744
- Rivkin, A. S., Thomas, C. A., Howell, E. S., & Emery, J. P. 2015, *AJ*, **150**, 14
- Rivkin, A. S., Davies, J. K., Johnson, J. R., et al. 2003, *M&PS*, **38**, 1383
- Russell, C. T., Raymond, C. A., Coradini, A., et al. 2012, *Sci*, **336**, 684
- Schmidt, B. E., & Castillo-Rogez, J. C. 2012, *Icar*, **218**, 478
- Shkuratov, Y., Starukhina, L., Hoffmann, H., & Arnold, G. 1999, *Icar*, **137**, 235
- Sierks, H., Lamy, P., Barbieri, C., et al. 2011, *Sci*, **334**, 487
- Takir, D., & Emery, J. P. 2012, *Icar*, **219**, 641
- Takir, D., Emery, J. P., McSween, H. Y., Hibbitts, C. A., & Clark, R. N. 2013, *M&PS*, **48**, 1618
- Tomeoka, K., Yamahana, Y., & Sekine, T. 1999, *GeCoA*, **63**, 3683
- Tonui, E., Zolensky, M., Hiroi, T., et al. 2014, *GeCoA*, **126**, 284
- Tyburczy, J. A., Frisch, B., & Ahrens, T. J. 1986, *E&PSL*, **80**, 201
- Urey, H. C. 1955, *PNAS*, **41**, 127
- Vernazza, P., Binzel, R. P., Thomas, C. A., et al. 2008, *Natur*, **454**, 858
- Vernazza, P., Carry, B., Emery, J., et al. 2010, *Icar*, **207**, 800
- Vernazza, P., Delbo, M., King, P. L., et al. 2012, *Icar*, **221**, 1162
- Vernazza, P., Marsset, M., Beck, P., et al. 2015, *ApJ*, **806**, 10
- Vernazza, P., et al. 2014, *ApJ*, **791**, 22
- Vickery, A. M. 1986, *Icar*, **67**, 224
- Vickery, A. M. 1987, *GeoRL*, **14**, 726
- Vilas, F., & Gaffey, M. J. 1989, *Sci*, **246**, 790
- Vilas, F., Larson, S. M., Hatch, E. C., & Jarvis, K. S. 1993, *Icar*, **105**, 67
- Vilas, F., & Sykes, M. V. 1996, *Icar*, **124**, 483
- Vincent, J.-B., Besse, S., Marchi, S., et al. 2012, *P&SS*, **66**, 79
- Walsh, K. J., Morbidelli, A., Raymond, S. N., O'Brien, D. P., & Mandell, A. M. 2011, *Natur*, **475**, 206
- Young, E. D. 2001, *RSPTA*, **359**, 2095
- Zolensky, M. E., Bourcier, W. L., & Gooding, J. L. 1989, *Icar*, **78**, 411
- Zolensky, M. E., Mittlefehldt, D. W., Lipschutz, M. E., et al. 1997, *GeCoA*, **61**, 5099
- Zolensky, M. E., Krot, A. N., Benedix, G., et al. 2008, *Reviews in Mineralogy and Geochemistry*, **68**, 429
- Zolensky, M. E., Mikouchi, T., Fries, M., et al. 2014, *M&PS*, **49**, 1997